IEEE Access
Multidisciplinary | Rapid Review | Open Access Journal

Received May 10, 2021, accepted May 28, 2021, date of publication June 9, 2021, date of current version June 24, 2021.

Digital Object Identifier 10.1109/ACCESS.2021.3087966

A Novel Highly-Efficient Amplification Scheme for Wireless Communications in a CathLab Environment

PEDRO VIEGAS[1], HUGO SERRA[2], JOÃO GUERREIRO[1,2,3], (Member, IEEE), RICARDO MADEIRA[3,4], DAVID BORGES[2], RUI DINIS[1,2,3], (Senior Member, IEEE), PAULO MONTEZUMA[1,2,3], (Member, IEEE), JOÃO PEDRO OLIVEIRA[1,3,4], (Member, IEEE), LUÍS M. CAMPOS[5], AND MARKO BEKO[2,6,7]

[1]Koala Tech, 2825-182 Monte da Caparica, Portugal
[2]Instituto de Telecomunica ções, 1049-001 Lisboa, Portugal
[3]FCT, Universidade Nova de Lisboa, 2829-516 Monte de Caparica, Portugal
[4]Uninova at FCT, 2829-516 Monte da Caparica, Portugal
[5]PDMFC, 1300-609 Lisboa, Portugal
[6]Instituto Superior Técnico, Universidade de Lisboa, 1049-001 Lisboa, Portugal
[7]Copelabs, 1700-097 Lisboa, Portugal

Corresponding authors: Pedro Viegas (pv@koalatech.pt) and João Guerreiro (jguerreiro.network@gmail.com)

This work was supported in part by Koala Tech through the support of P2020—Projetos Individuais—Internacionalização under Grant LISBOA-02-0752-FEDER-038713, in part by the Fundação para a Ciência e Tecnologia, in part by the Instituto de Telecomunicações under Project UIDB/50008/2020 and the Project PES3N under Grant POCI-01-0145-FEDER-030629, and in part by the POSITION II through the Electronic Component Systems for European Leadership Joint Undertaking (ECSEL-JU) under Grant 783132-Position-II-2017-IA.

ABSTRACT Wireless communication systems are being considered for medical applications to facilitate the doctors' operation and the quality of the medical procedures. A demonstrative example of this is the catheterization laboratory (CathLab), where it is desirable to replace the existent wired connections by wireless alternatives. However, there are some challenging requirements that need to be fulfilled by the wireless link, especially for intra-vascular ultra-sound (IVUS) systems, since the images acquired by the catheter should be transmitted with very high data rate and low latency, together with the highest possible amplification efficiency, to increase the battery life. The communication requirements can be achieved with latest the Wi-Fi standard IEEE 802.11ax (Wi-Fi 6). However, since Wi-Fi is based on orthogonal frequency division multiplexing (OFDM) waveforms, the transmitted signals present high envelope fluctuations, leading to amplification difficulties due to the nonlinear distortion effects and low energy efficiency. In this paper, we present an innovative amplification scheme named quantized digital amplification (QDA). It is shown that the QDA allows a quasi-linear amplification of IEEE 802.11ax signals while maintaining a very high energy efficiency. To demonstrate this, a QDA prototype and a set of performance results, regarding both the linearity of the transmitted signals and the energy efficiency, are presented.

INDEX TERMS CathLab, Wi-Fi, orthogonal frequency division multiplexing, peak-to-average power ratio, power amplification.

I. INTRODUCTION

Medical procedures and tools are constantly evolving with new technologies. An example of this are the IVUS systems for image acquisition in CathLab, where powerful millimeter-sized ultrasounds and cameras are able to provide high-resolution images with low latency, which are suitable for IVUS operations [1]. In a conventional CathLab, the images acquired by the different catheters are transmitted through a wired connection, which introduces a significant amount of cables in the vicinity of the stretcher, increasing the complexity of the procedure and complicating the sterilization processes [2], [3]. In that context, the adoption of wireless communications would be a solution for this problem, since most of the cables could be removed [4]. However, this alternative should fulfill the communication requirements of

The associate editor coordinating the review of this manuscript and approving it for publication was Donatella Darsena.

the catheterization laboratory (Cathlab). Devices that require low rate communications like fractional flow reserve (FFR) are not difficult to turn wireless. However, turning wireless devices like the IVUS that involve reliable very high data rates (from 300 Mbps to 1 Gbps) and low latency (less than 100 ms), together with demanding quality of service (QoS) parameter, can present a significant challenge [5].

The latest standard of wireless local area networks (WLANs) IEEE 802.11ax (also known as Wi-Fi 6) can achieve these transmission rates and latency values, namely by adopting multiple antenna techniques (i.e., advanced multi-user multiple-input, multiple-output (MIMO) schemes), large bandwidths and large constellations [6]. Wi-Fi 6 is supported by highly spectral-efficient OFDM waveforms [7]. However, it is widely known that OFDM signals present a very large peak-to-average power ratio (PAPR), since they are formed by the sum of several independently modulated subcarriers [8]. This yields a challenging trade-off between energy efficiency and nonlinear distortion, since the most energy-efficient power amplifiers (PAs) are known to exhibit a strong nonlinear characteristic [9]. Since wireless devices used in the CathLab context cannot have large dimensions, the design of their batteries is highly constrained. Under these conditions, it is highly important to have improved energy efficiency, so as to improve the battery life.

Several techniques have been proposed to improve the efficiency of PAs, such as: envelope elimination and restoration (EER) [10]–[13]; predistortion [14], [15]; Doherty PA [16]–[18]; linear amplification with nonlinear control (LINC) [19], [20]; and envelope tracking (ET) [21]–[23]. The EER technique uses a combination of a switching-mode PA and an envelope demodulation circuit. The efficiency of this technique, which is the product between the efficiencies of the envelope amplifier (EA) and the radio frequency (RF) PA, greatly depends on the performance of the EA, since a degradation in the EA's efficiency can negate any improvements achieved in the RF PA's efficiency. In the Doherty PA architecture the carrier amplifier, which is terminated with an impedance load at twice the optimum value, is a Class B or AB amplifier, supplying the load with current for any input power level, while the peaking amplifier should only switch ON when the main amplifier reaches saturation. The output current will then modulate the load seen by the carrier amplifier from twice the optimum value to the optimum value. Using this approach it is possible to achieve higher efficiency levels. However, there are limitations in terms of usable bandwidth, the amplifiers need to be linear to prevent distortion, and the design can be quite complex to achieve optimum performance. In the LINC technique the input signal is decomposed into two constant envelope signals, which are then amplified separately by two highly efficient non-linear amplifiers (e.g., of class D or E) to achieve the desired output power and combined together in a power combining network. The output amplitude can be controlled via the relative phase of the two constituent signals. However, LINC transmitter scheme is limited by the input signal's envelope characteristics. Since the amplitude information of the band-limited signal is embedded in the phase of the LINC components, a highly fluctuating envelope produces a constant envelope LINC component with high phase content, which causes the LINC components' spectrum to spread. Another problem is how the power combining is done, particularly because several high efficiency power amplifiers are highly sensitive to load impedance, and their performance and efficiency can be significantly degraded due to interactions between the power amplifiers. The ET technique uses a linear PA and a supply modulation circuit, where the supply voltage tracks the input envelope. By replacing the fixed supply with the dynamic supply voltage, the DC power consumption of an ET PA can be reduced, when compared with a conventional PA, increasing its efficiency. More specifically, the power that is supplied to the amplifier is changed to be just enough to reproduce the power level required by the amplifier at a given instant of time. For low output power, the supply voltage is reduced, and for high output powers it is increased. However, while ET amplifiers are easier to design, they provide smaller efficiency benefits than their EER counterparts, since linear RF PAs need to be used. Recently, a promising amplification technique named QDA was proposed to solve the trade-off between power efficiency and nonlinear distortion [24], [25]. This technique involves the decomposition of high-PAPR signals into almost constant-envelope components, that can be independently amplified by highly-efficient, switched PAs and that can be digitally combined afterwards. It was shown that when employed with OFDM, the QDA can increase the energy efficiency of the amplification process up to 40% [25]. In this work, we consider the use of QDA in the context of a Wi-Fi link associated to a wireless CathLab. We present a QDA prototype and a set of performance results regarding the energy efficiency, the power spectral density (PSD), the error vector magnitude (EVM) and the bit error rate (BER) of the transmitted signals. It is shown that the QDA can be an excellent solution for the amplification of CathLab wireless signals in general, and IVUS signals in particular, providing an energy-efficient operation with negligible distortion on the transmitted signals.

II. SYSTEM CHARACTERIZATION

A. CathLab ENVIRONMENT

Let us start by describing the wireless communication scenario considered in this work. Essentially, we consider a Cathlab scenario similar to the one represented in Fig. 1, which shows the Philips CathLab®.

The catheter is connected to the patient interface module (PIM), which transmits the captured images to the receiver installed in the stretcher. We will focus on the IVUS communications, although our work can be employed with any CathLab device that requires wireless communications, such as for instance the FFR. For the wireless link that support the IVUS, we consider a Wi-Fi connection supported by the IEEE WLAN 802.11ax standard. In the considered scenario,

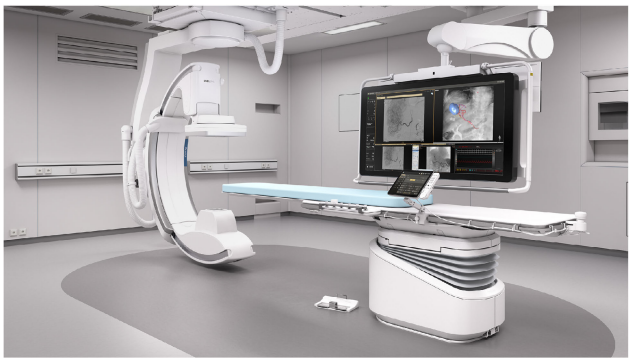

FIGURE 1. Philips CathLab ®.

the PIM (i.e., the transmitter) acts as a Wi-Fi station (STA), while the receiver located in the stretcher is the Wi-Fi access point (AP). Therefore, we are concerned with uplink communications.

B. WI-FI COMMUNICATION ASPECTS & PROBLEM STATEMENT

One of the innovative aspects of IEEE 802.11ax is the use of orthogonal frequency division multiple access (OFDMA) for both downlink and uplink channels [6], which allows an efficient resource allocation and users' scheduling. In Wi-Fi 6, the achievable data rates per spatial stream (SS) are mainly dependent on: (i) the channel bandwidth, B; (ii) the size of the quadrature amplitude modulation (QAM), M; and (iii) the adopted code rate. For instance, by combining a bandwidth of $B = 80$ MHz with 64-QAM constellations and a code rate 5/6, it is possible to achieve $R = 360$ Mbps [6]. Since the capacity gains provided by the use of MIMO in the Wi-Fi-based CathLab applications might not be as high as expected by the theory due to correlations between MIMO antennas [5], an alternative to increase the data rates per SS might resort to the adoption of larger constellations (i.e., higher values of M). However, this will increase even more the (already high) envelope fluctuations of the transmitted OFDM signals, as well as the sensitivity to hardware imperfections and nonlinear distortions, causing severe amplification issues. Under these conditions, a linear amplification can only be obtained by employing PAs with large back-offs, which drastically reduces the energy efficiency of the amplification process [9].

The QDA constitutes a solution to these amplification issues, since the high-PAPR signal is divided into low-PAPR components that can be amplified by high energy-efficient, switched PAs (such as the ones of class D or E) without distorting the transmitted signals. Therefore, the overall energy efficiency of the transmitter can be greatly increased, even when signals with very large PAPR are considered.

III. QDA PRINCIPLES AND SIGNALS DESCRIPTION

In this section, the QDA principles and main aspects are explained. The general scheme of the QDA is shown in Fig. 2.

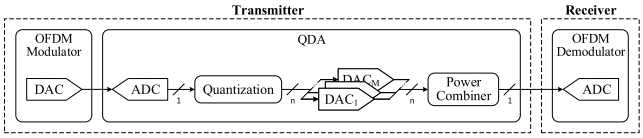

FIGURE 2. General scheme of the QDA.

Let us start by considering the complex envelope of a given OFDM signal, $\bar{x}(t)$, which has bandwidth $B/2$ and is formed by N subcarriers. The first step associated to the QDA's operation is to mix $\bar{x}(t)$ to an intermediate frequency f_i, which originates the pass-band signal $x(t) = \bar{x}(t)\sin(2\pi f_i t)$ with bandwidth B. This signal is then sampled with a sampling frequency f_s, yielding the time-domain samples $x_n = x(nT_s)$, where $T_s = 1/f_s$ is the sampling time and n is the time instant index. The next steps of the QDA's operation involves three main stages, namely the quantization stage, the amplification stage and the combining stage. These stages are described in the following subsections.

A. QUANTIZATION STAGE

In this stage, the time-domain samples x_n are quantized by an uniform quantizer characterized by the nonlinear function $h(\cdot)$ (the extension to non-uniform quantizers is straightforward). We consider M quantization bits and $Q = 2^M$ levels. The clipping level of the quantization characteristic is selected to minimize the overall quantization distortion [26]. The normalized clipping level is represented by s_M/σ, where $\sigma = 0.5\sqrt{|\bar{x}(t)|^2}$ is the standard deviation of the $x(t)$.

The digital word associated to the n^{th} time-domain sample is $\underline{b}_n = \{b_{n,1}, b_{n,2}, \ldots, b_{n,M}\} = h(x_n)$. This digital word has two main functions:

(i) Control the bank of M digital-to-analog converters (DACs) that follow the quantization procedure and are responsible to generate the different binary phase shift keying (BPSK) signal components that will be amplified and combined;

(ii) To be used to generate the control bits ($d_{n,1}, d_{n,2}, \ldots, d_{n,3(M-1)}$), responsible for the control of the switching process at the combining stage.

Since each BPSK component can be designed to have a quasi-constant-envelope, it is possible to use nonlinear and highly-efficient switched PAs, avoiding the signal distortion associated to the nonlinear effects of the PAs. The signals generated by the M BPSK modulators are then combined to form the desired amplitude for each given sample. The m^{th} BPSK signal component produced by the DAC can be described as

$$s_m(t) = A_m \sin(2\pi f_c t + \phi_m), \tag{1}$$

where $A_m = \sqrt{k_{(2^m-1)} \times P}$ (with P denoting the "basis" power level in Watts (W)) represents the amplitude, f_c represents the carrier frequency, and ϕ_m represents the phase of each component (which can assume the 0 or π values, depending on the polarity of the input sample).

B. AMPLIFICATION STAGE

Depending on the QDA version, this stage can be present or not. For some wireless applications in the CathLab with low power requirements (e.g. applications designed for FFR), it might not be necessary to have an external amplification stage, i.e., the DACs from the field programmable gate array (FPGA) are enough to yield the desired output power. In those scenarios, the QDA is said to operate in the ''fully-digital'' regime. However, there are some applications that require higher power levels, such as the wireless transmission of IVUS signals. In such applications, a bank of M highly-efficient switched PAs (such as the ones of class D, E or F) can be employed after the quantization stage, resulting in an ''hybrid'' version of the QDA. In that scenario, it should be noted that each one of these M PAs can be enabled or disabled depending on the digital word associated to a given sample.

C. COMBINING STAGE

The combining stage is associated to the ''digitally-controlled smart combiner (DCSC)'' block of the QDA and its operation is controlled by the digital word generated by the quantization process. In Fig. 3 it can be observed the relation between the power level of a given quantized sample and the digital word associated to it, which also controls the combination of the BPSK components. It is important to mention that Fig. 3 is associated to a 4-bit quantizer, i.e., $Q = 2^M = 16$ quantization levels.

Binary Power				Corresponding Power Level
P	2P	4P	8P	
1	1	1	1	k_{15} P
0	1	1	1	k_{14} P
1	0	1	1	k_{13} P
0	0	1	1	k_{12} P
1	1	0	1	k_{11} P
0	1	0	1	k_{10} P
1	0	0	1	k_9 P
0	0	0	1	k_8 P
1	1	1	0	k_7 P
0	1	1	0	k_6 P
1	0	1	0	k_5 P
0	0	1	0	k_4 P
1	1	0	0	k_3 P
0	1	0	0	k_2 P
1	0	0	0	k_1 P
0	0	0	0	k_0 P

FIGURE 3. Relation between the digital words associated to the Q quantization levels and the corresponding power of the combined signal when $M = 4$.

For the hybrid version of the QDA, the output signal of the DCSC at n^{th} time instant can be written as

$$y_n(t) = \sum_{m=1}^{M} b_{n,m} G_m s_m(t). \tag{2}$$

where G_m represents the gain of the m^{th} PA. When taking into account the signal's evolution over a certain interval of time (i.e., several time-domain samples of the underlying bandpass signal $x(t)$), the combined signal at the combiner's output can be represented as

$$y(t) = \sum_{n=-\infty}^{+\infty} y_n(t - nT_s), \tag{3}$$

where n represents the time index and T_s the symbol time interval. Note that the combining stage is also important in what concerns to the overall QDA energy efficiency, since the signals' combination is made according to the control bits $(d_{n,1}, d_{n,2}, \ldots, d_{n,3(M-1)})$ associated to the digital word $\underline{b}_n = \{b_{n,1}, b_{n,2}, \ldots, b_{n,M}\}$.

IV. QUANTIZED DIGITAL AMPLIFICATION PROTOTYPE

In this section, we present a prototype of the hybrid version of the QDA. The general scheme of this prototype is shown in Fig. 4. The QDA receives an OFDM signal generated with a GNURadio Companion flowgraph (OFDM TX example from gr-digital package of GNURadio 3.9 PPA), which is sent by an universal software radio peripheral (USRP), model Ettus N210 from National Instruments. After the QDA operation, the signal is then transmitted to another Ettus N210 (which acts as the receiver), where the GNURadio Companion demodulates the received signal by taking into account another flowgraph of the gr-digital package, designated as OFDM RX example.

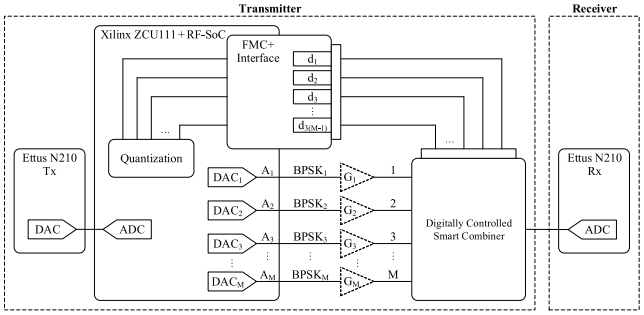

FIGURE 4. General scheme of the QDA operating in an OFDM transceiver.

The hardware and software tools used to implement and evaluate the QDA will be further detailed in this section. In what concerns to the QDA prototype, both the ''fully-digital'' and the ''hybrid'' versions will be presented and analyzed. In both cases, it was considered $M = 4$ quantization bits (i.e., $M = 4$ amplification branches). The fully-digital version of the QDA can be observed in Fig. 5, where it can be noted that the DACs are directly connected to the DCSC. On the other hand, the ''hybrid'' version of the QDA prototype can be observed in Fig. 6. In this version, the DACs' outputs are connected to the amplifiers before being sent to DCSC.

A. HARDWARE & IMPLEMENTATION ASPECTS

As shown in Fig. 4, the QDA is composed of a Xilinx ZCU111 + RF-SOC evaluation kit and three printed circuit

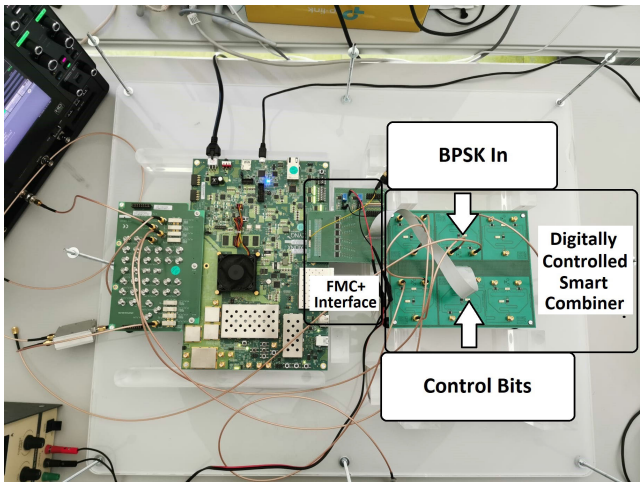

FIGURE 5. Prototype of the fully-digital version of the QDA [25].

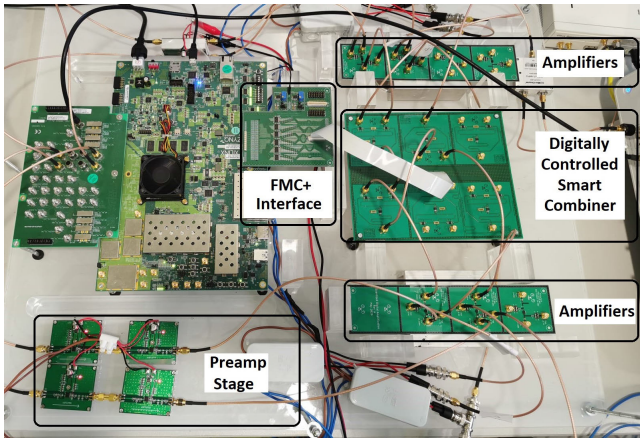

FIGURE 6. Prototype of the hybrid version of the QDA.

boards (PCBs), namely the FMC+ interface card PCB (used to send the control bits from the Xilinx board to the Koala Tech's DCSC), the DCSC PCB, and the PCB of the amplification stage, which is formed by an array of several class-E PAs. The DCSC and FMC+ interface card PCBs are shown in Fig. 7.

The PCB of the amplification stage (which can be present or not, depending on the power requirements of the system) is shown in Fig. 8.

The Class-E PAs represented in the figure were designed by Koala Tech and present high energy efficiencies, up to approximately 70%.

In what concerns to the signal parameters adopted for this implementation, the QDA prototype was tested with an OFDM modulation with bandwidth $B = 250$ kHz[1] and $N = 64$ subcarriers with 16-QAM constellations. The considered sampling frequency was $f_s = O \times B = 2$ MHz, so as to guarantee oversampling factor $O = 8$.[2] The adopted carrier frequency was $f_c = 880$ MHz.

[1]The on-chip implementations of the QDA will allow bandwidths up to $B = 200$ MHz.

[2]The latest optimized implementations of QDA do not have an oversampling factor.

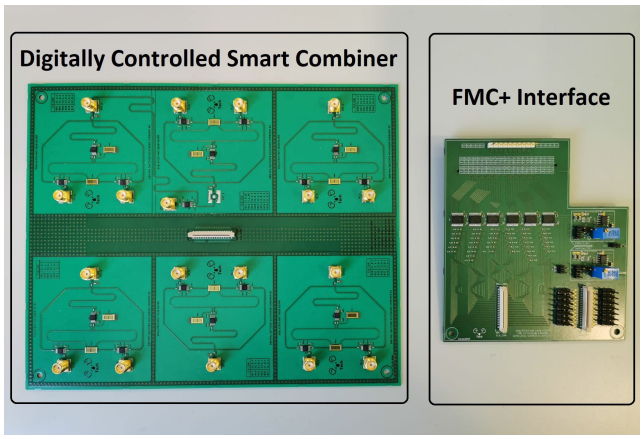

FIGURE 7. Koala Tech's FMC+ Interface Card and DCSC.

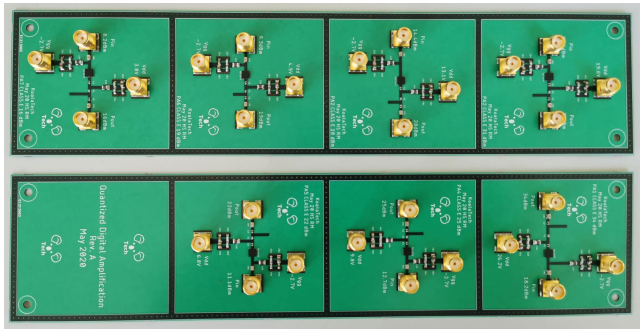

FIGURE 8. Koala Tech's amplification stage PCB composed by Class-E PAs.

B. PCB IMPLEMENTATION & DESIGN

1) POWER AMPLIFIER ARRAY

As discussed in the previous section, the PA array is composed by 4 individual Class-E PAs [29] (PA_1, PA_2, PA_3, and PA_4) optimized for an output power of 16, 19, 22, and 25 dBm, respectively, at $f_c = 880$ MHz. These were implemented using the Qorvo TGF2977 transistor and off-the-shelf capacitors and inductors to implement the circuit shown in Fig. 9. The PAs were designed with load-pull and electromagnetic simulations using the AWR Design Environment and the component's models from Modelithics. The supply voltages (V_{DD}), capacitor's, and inductor's values are different between the PAs, whilst the schematic remains the same for all, as well as the V_{GG} voltage, which is equal to -2.7 V.

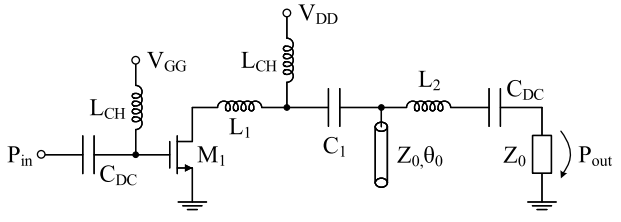

FIGURE 9. Simplified schematic of the class-E PA with the highest power value.

Fig. 10 shows the measurement results of each PA's power added efficiency (PAE) as a function of the output power

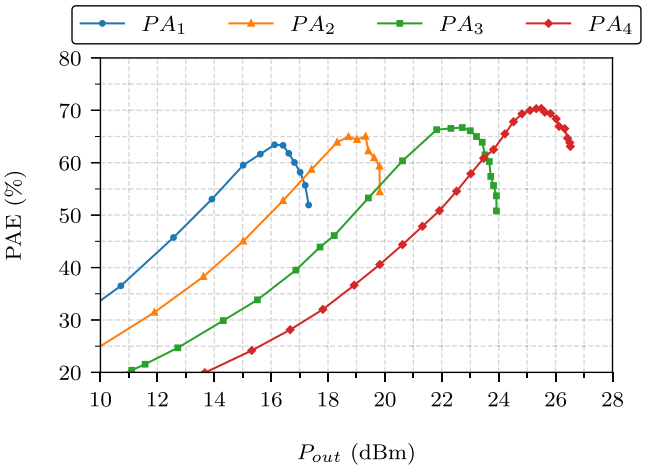

FIGURE 10. Measured P_{out} and PAE of the four Class-E PA array.

TABLE 1. PA array performance at the desired output power level.

PA #	V_{DD}	P_{in} (dBm)	P_{out} (dBm)	PAE (%)
1	3.21	6.2	16	63.4
2	5.64	8.6	19	64.4
3	8.26	9.1	22	66.4
4	12.29	10.3	25	69.7

(P_{out}), where $PAE = (P_{out} - P_{in})/P_{DC}$. The graph shows that each PA reaches the maximum PAE at the designed output power. The PAE values are approximately between 63% and 70%, with a weighted average value of 67%. Table 1 shows values of the supply voltage, input and output power, and PAE, at the desired output power, for each PA of the PA array.

2) DIGITALLY CONTROLLED SMART COMBINER

The smart combiner is implemented using $M - 1$ power combining sections connected in a ladder structure, where the combiner is based on the Wilkinson power combiner topology [30], using RF single pole double throw (SPDT) switches at the inputs and at the output to allow reconfigurability, depending on the presence or absence of signals at the inputs of the combiner. The digitally controlled Wilkinson power combiner is shown in Fig. 11. When both inputs of the combiner have signals present ($P_{in1,2} \neq 0$), the SPDT switches at the input connect to the isolation resistance R_{isol} and the SPDT switch at the output connects to the output P_{out}, i.e., when both signals are present, the circuit behaves as a typical Wilkinson power combiner. When only one signal is present, the SPDT switch with the signal will connect to the output P_{out}, while the other input SPDT switch connects to the isolation resistance and the output SPDT switch connects to the Z_0 resistance, i.e., in this configuration the combiner acts as a bypass circuit, avoiding the loss of half the power that would occur in the Wilkinson power combiner when combining a signal with zero. Finally, when no signal is present at both inputs, the input SPDT switches connect to the isolation resistance and the output SPDT switch connects to the Z_0 resistance, i.e., the combiner will be in an idle state.

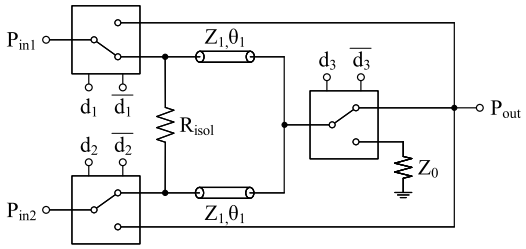

FIGURE 11. Simplified schematic of the digitally controlled Wilkinson power combiner.

Note that in Fig. 11, $R_{isol} = 2Z_0$, $Z_1 = \sqrt{2}Z_0$, and $\theta_1 = \lambda/4$, where Z_0 represents the circuits characteristic impedance and λ is the wavelength. It is also important to mention that the switches were implemented using Analog Devices' HMC190BMS8 SPDT switch. The digital signals d_1, d_2, and d_3 control the SPDT switches and are set by the FPGA. The FMC+ interface board is responsible for shifting these signals voltages (1.8 V) to the appropriate switch voltage (5 V), using level shifters. The correspondence between the configuration bits and the combiner state is summarized in Table 2.

TABLE 2. Smart combiner control bits.

Combiner state	P_{in1}	P_{in2}	d_1	d_2	d_3
Idle	$= 0$	$= 0$	1	1	0
Bypass P_{in1}	$\neq 0$	$= 0$	0	1	0
Bypass P_{in2}	$= 0$	$\neq 0$	1	0	0
Combine	$\neq 0$	$\neq 0$	1	1	1

Starting the combination from the lowest power to the highest power, and using the previously described combiner configurations, it is possible to combine signals with minimum power loss. The resulting average combination efficiency for four signals with the output powers shown in Table 1 was 46.5%.[3]

V. PERFORMANCE RESULTS

The QDAs's performance evaluation should consider different aspects, such as the power efficiency, which can be measured by the PAE, as well as other important performance aspects related to the communication performance, which includes the PSD, EVM and the BER.

GNURadio tools were used to measure the EVM and the signal's constellation. Moreover, an oscilloscope was employed to analyze the PSD of the combined signal at the QDA output. The presented results are similar on both QDA versions (i.e., for the "fully-digital" and "hybrid" versions), differing only on the power efficiency. In fact, the power efficiency for the hybrid version is 20% lower than the one associated to the fully-digital version, which can be explained by the PAE of the PAs ($\approx$ 70%).

[3]Actually, even higher combination efficiencies have been observed in optimized versions of the DCSC that are currently in their last stages of development.

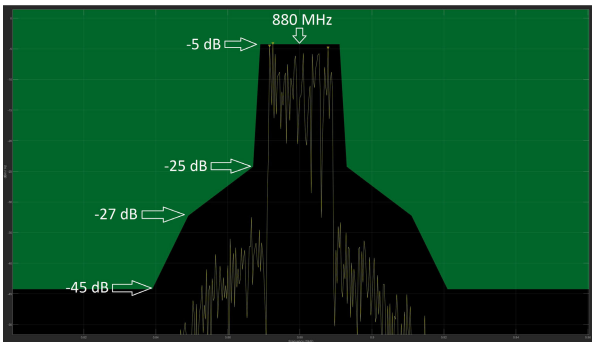

FIGURE 12. PSD of the combined signal with $M = 4$ components and the Wi-Fi spectral mask.

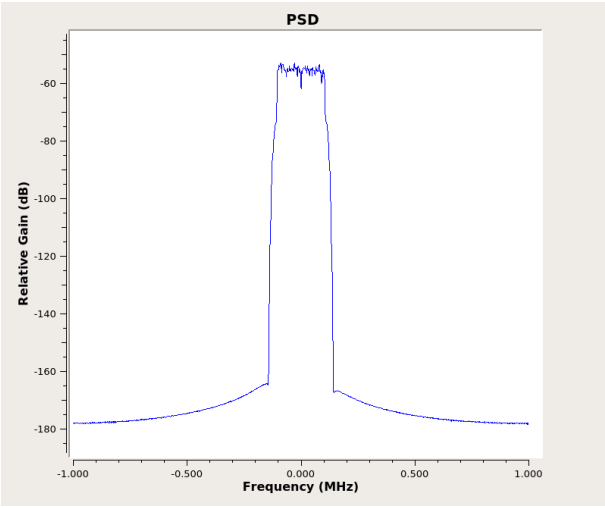

FIGURE 13. PSD of the combined signal measured with the GNU radio software.

A. QDA ENERGY EFFICIENCY

The overall energy efficiency average of this QDA prototype is approximately 31.3%.[4] This energy efficiencies were calculated by the average products between the weighted average PAE of the Class-E PA array and the average efficiency of the DCSC, for each of the Q codes.

B. PSD

The PSD is one of the important performance parameters to be analyzed, since all transmission systems must be fully compliant with the spectral mask of the underlying wireless communication standard. This parameter allows to observe the out-of-band (OOB) distortion of the transmitted signal. In Fig. 12, it can be observed that the QDA is compliant with the spectral masks of Wi-Fi.

Some additional measurements were also made using the GNU Radio software, namely to analyze the PSD of the combined signal, which is shown in Fig. 13.

In Fig. 14 can be observed the obtained PSD on the oscilloscope, which confirm the results presented above.

[4]This energy efficiency is also higher with the optimized version of the DCSC ($\approx 50\%$).

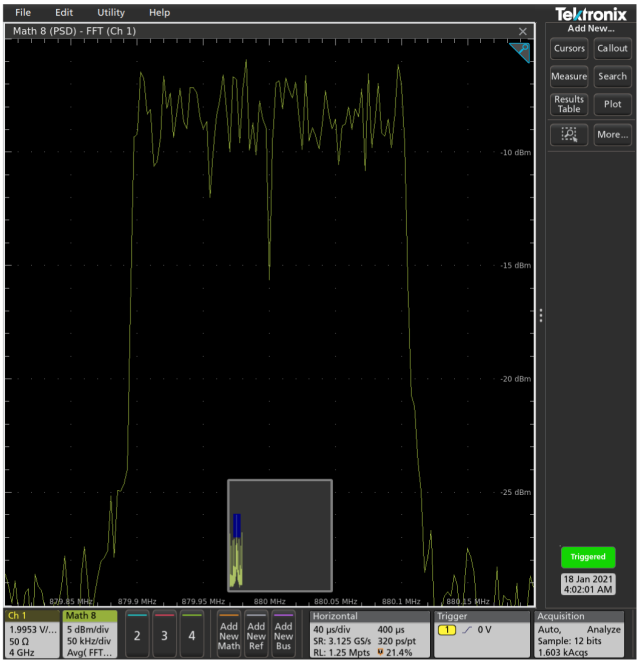

FIGURE 14. PSD of the combined signal measured in the oscilloscope.

C. EVM

The EVM parameter is related to the signal's integrity in the in-band region, which is also related to the signal's constellation. The constellation diagram after the QDA operation can be seen in Fig. 15.

In Fig. 15, it can be noted that the differences between the original constellation and the one produced by the QDA prototype are small. This can be verified by computing the EVM, which is given by [28]

$$\mathrm{EVM}_{RMS} = \sqrt{\frac{\frac{1}{N}\sum_{m=1}^{N} e_m}{\frac{1}{N}\sum_{m=1}^{N}(I_m^2 + Q_m^2)}} \times 100, \qquad (4)$$

where $e_m = (I - \tilde{I}_m)^2 + (Q - \tilde{Q}_m)^2$, with I and Q denoting the original constellation values, and $\tilde{I}_m$ and $\tilde{Q}_m$ represent the received symbols at the m^{th} OFDM subcarrier. The EVM calculated with (4) was approximately 5 % for both versions of the prototype (i.e., for the fully-digital and the hybrid versions).

TABLE 3. EVM compliance of the QDA for the constellation sensitivity standards [27], [31].

QDA		EVM Compliance				
M	EVM_{RMS} (%)	QPSK (17,5%)	16-QAM (12,5%)	64-QAM (8%)	256-QAM (3,5%)	1024-QAM (2,5%)
4	4,5	✓	✓	✓	✗	✗
5	3	✓	✓	✓	✓	✗
6	2	✓	✓	✓	✓	✓
7	1,5	✓	✓	✓	✓	✓
8	1	✓	✓	✓	✓	✓

Let us consider Table 3, which shows the simulated the EVM values of the QDA considering a different number

TABLE 4. Measurement summary and comparison with other architectures found in the literature.

		This Work	RFIC'20 [32]		TCASI'20 [33]	JSSC'16 [34]	JSSC'15 [35]	ISSCC'17 [36]		MWCL'14 [37]	ISSCC'10 [38]	ISSCC'10 [39]
	Freq. (MHz)	**880**	28000		2400	3710	1900	4900/5900		16500	60000	60000
	BW (MHZ)	**0.25**	4000		10	1000	20	160		N.A.	N.A.	N.A.
	Technology	**Discrete**	22 nm FDSOI		45 nm CMOS	65 nm CMOS	40 nm CMOS	55 nm CMOS 180 nm SOI		180 nm BiCMOS	90 nm CMOS	65 nm CMOS
	Architecture	**QDA**	TRX front end module		Multi-mode outphasing	Class G mixed-signal Doherty PA	Dual-mode Doherty PA	Doherty PA		2-stage cascode and Wilkinson divider/combiner	2-stage PA and Wilkinson divider/combiner	N-way differential power combiner (transformer)
	Supply (V)	**12.3/3.2**	2.4/0.8		2.4	3	1.5	3.3		2.4	1.8	0.9/1.0
PA	Gain (dB)	**9.8/14.35**	30		N.A.	N.A.	N.A.	26		34.5	26.1	18.9/19.2
PA	PAE (%)	**63.4 (9 dB BO)**	8.7 (6 dB BO)		25.3 (6 dB BO DE SLO) 32.9 (6 dB BO DE AMO)	37.0 (6 dB BO DE)	25.5 (6 dB BO)	N.A.		N.A.	N.A.	N.A.
PA		**69.7****	21.5**		49.2** (DE)	40.2** (DE)	34**	N.A.		17	10.5**	10.8/11.1**
SYSTEM	Signal Modulation	**16 QAM**	64 QAM	256 QAM	64 QAM LTE	16 QAM	16 QAM LTE	MCS 9	MCS 11	N.A.	N.A.	N.A.
SYSTEM	Data Rate (MHz)	**2**	2400	800	N.A.	N.A.	N.A.	N.A.	N.A.	N.A.	N.A.	N.A.
SYSTEM	EVM (dB)	**-27**	-25	-30	-39.4 (SLO) -25.2 (AMO)	-24	-23	-35	-38	N.A.	N.A.	N.A.
SYSTEM	Pout (dBm)	**21.8***	11.13*	10.1*	31.6**	26.7**	28**	20.3	18.3	18.3	14.5**	17.6 (PSAT)
SYSTEM	PAE (%)	**31.3***	9.7*	8.3*	N.A.	N.A.	N.A.	12***	10***	N.A.	N.A.	N.A.

*Average value, **Maximum value, ***At the desired P_{out} value, N.A. not available, DE: Drain Efficiency, SLO: Single Level Outphasing, AMO: Asymmetric Multilevel Outphasing, BO: Backoff, MCS: Multilevel Coded Spreading Symbols.

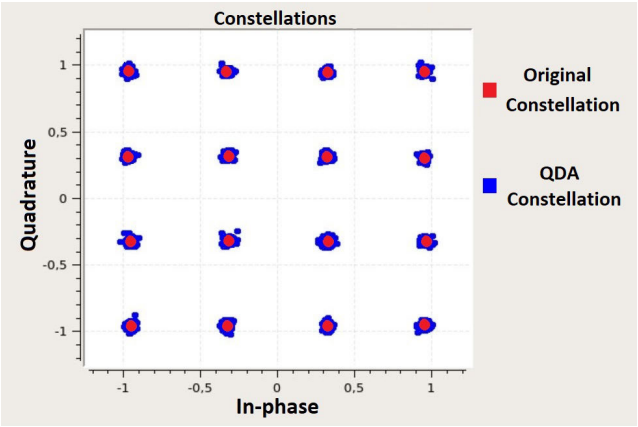

FIGURE 15. Original 16-QAM constellation and received constellation after the QDA's operation.

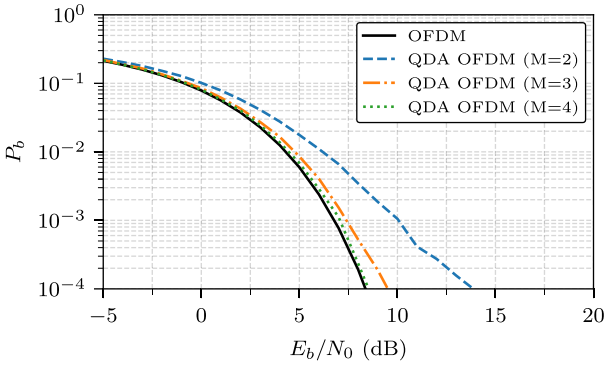

FIGURE 16. Simulated BER performance of a nonlinear OFDM system.

quantization bits and different constellations. From the analysis of those values, it can be noted that the prototype met the EVM value for 64-QAM constellations required for Wi-Fi applications.[5] Moreover, it can be observed that when $M = 6$ quantization bits are considered, the QDA can support even larger constellations. This demonstrates that the in-band distortion caused by the QDA prototype is very low and that besides it exhibits a very high energy efficiency, it does not compromise the linearity of the transmitted signals.

D. BIT ERROR RATE

The BER is another important performance result to be evaluated. In what concerns to the BER evaluation of the QDA, it can be concluded that the main distortion introduced by the QDA is the quantization error, which can be interpreted as an additional noise component. The quantization noise decrease as the number of quantization bits increases, reducing the number of errors occurred and consequently improving the BER curve. This effect can be seen in Fig. 16, which shows the simulated BER of a nonlinear OFDM system with a quantization process, with M quantization bits.

As can be seen in Fig. 16, the BER is denoted as P_b and it is plotted as a function of E_b/N_0, where E_b is the average bit energy and N_0 is the one-sided additive white Gaussian noise (AWGN) PSD. From the same figure, it can be observed that with $M = 2$ quantization bits there is a considerable performance degradation. On the other hand, with $M \geq 3$, the impact of the quantization noise in the system performance is minimal.

In Table 4, the performance measurements of other techniques were compared with the ones of the QDA prototype presented on this work.

VI. CONCLUSION

In this work, a wireless CathLab based on the IEEE 802.11ax standard was considered. To tackle the well-known amplification issues associated to conventional Wi-Fi transmitters, a novel amplification scheme based on the decomposition of the Wi-Fi OFDM signal into several low-PAPR components, which are individually amplified and digitally combined, is presented. It is shown that the QDA is adequate for different use cases in the wireless CathLab, ranging from low power applications such as FFR and high-power applications such as wireless IVUS. In the latter case, an external amplification

[5]The EVM produced by the QDA prototype is also compliant with requirements of 4G/5G standards

stage based on highly-efficient PAs can be easily integrated into the QDA. Moreover, we presented a QDA prototype and a set of performance results, being demonstrated that a large energy efficiency can be obtained without compromising the linearity of the transmitted signals. Therefore, the QDA can be an excellent solution for the amplification of wireless CathLab signals.

ACKNOWLEDGMENT

This work was supported by Koala Tech, under the support of P2020 - Projetos Individuais - Internacionalização, (LISBOA-02-0752-FEDER-038713), by Fundação para a Ciência e Tecnologia and Instituto de Telecomunicações under projects UIDB/50008/2020 and PES3N (POCI-01-0145-FEDER-030629) and by POSITION II, which received funding from the Electronic Component Systems for European Leadership Joint Undertaking (ECSEL-JU) under grant agreement 783132-Position-II-2017-IA.

REFERENCES

[1] A. Katouzian, E. D. Angelini, S. G. Carlier, J. S. Suri, N. Navab, and A. F. Laine, "A state-of-the-art review on segmentation algorithms in intravascular ultrasound (IVUS) images," *IEEE Trans. Inf. Technol. Biomed.*, vol. 16, no. 5, pp. 823–834, Sep. 2012.

[2] R. Stoutea, M. C. Louwersea, J. van Rensb, V. A. Hennekenb, and R. Dekker, "Optical data link assembly for 360 μ m diameter IVUS on guidewire imaging devices," in *Proc. IEEE Sensors*, Valencia, Spain, Nov. 2014, pp. 217–220.

[3] H. Sharei, R. Stoute, J. J. van den Dobbelsteen, M. Siebes, and J. Dankelman, "Data communication pathway for sensing guidewire at proximal side: A review," *J. Med. Devices*, vol. 11, no. 2, Jun. 2017, Art. no. 02450.

[4] S. G., R. R. Chittal, and K. Kumar, "Medical applications of wireless networks," in *Proc. 2nd Int. Conf. Syst. Netw. Commun. (ICSNC)*, Aug. 2007, p. 82.

[5] J. Guerreiro, R. Dinis, and L. Campos, "On the achievable capacity of MIMO-OFDM systems in the CathLab environment," *Sensors*, vol. 20, no. 3, p. 938, Feb. 2020.

[6] E. Khorov, A. Kiryanov, A. Lyakhov, and G. Bianchi, "A tutorial on IEEE 802.11ax high efficiency WLANs," *IEEE Commun. Surveys Tuts.*, vol. 21, no. 1, pp. 197–216, 1st Quart., 2019.

[7] D. Bankov, A. Didenko, E. Khorov, and A. Lyakhov, "OFDMA uplink scheduling in IEEE 802.11ax networks," in *Proc. IEEE Int. Conf. Commun. (ICC)*, May 2018, pp. 1–6.

[8] H. Ochiai and H. Imai, "On the distribution of the peak-to-average power ratio in OFDM signals," *IEEE Trans. Commun.*, vol. 49, no. 2, pp. 282–289, Feb. 2001.

[9] J. Joung, C. K. Ho, and S. Sun, "Spectral efficiency and energy efficiency of OFDM systems: Impact of power amplifiers and countermeasures," *IEEE J. Sel. Areas Commun.*, vol. 32, no. 2, pp. 208–220, Feb. 2014.

[10] L. Kahn, "Single-sideband transmission by envelope elimination and restoration," *Proc. IRE*, vol. 40, no. 7, pp. 803–806, Jul. 1952.

[11] F. Wang, D. Kimball, J. Popp, A. Yang, D. Y. C. Lie, P. Asbeck, and L. Larson, "Wideband envelope elimination and restoration power amplifier with high efficiency wideband envelope amplifier for WLAN 802.11g applications," in *IEEE MTT-S Int. Microw. Symp. Dig.*, Jun. 2005, pp. 645–648.

[12] F. Wang, A. H. Yang, D. F. Kimball, L. E. Larson, and P. M. Asbeck, "Design of wide-bandwidth envelope-tracking power amplifiers for OFDM applications," *IEEE Trans. Microw. Theory Techn.*, vol. 53, no. 4, pp. 1244–1255, Apr. 2005.

[13] C.-T. Chen, Y.-C. Lin, T.-S. Horng, K.-C. Peng, and C.-J. Li, "Kahn envelope elimination and restoration technique using injection-locked oscillators," in *IEEE MTT-S Int. Microw. Symp. Dig.*, Jun. 2012, pp. 1–4.

[14] L. Ding, G. T. Zhou, D. R. Morgan, Z. Ma, J. S. Kenney, J. Kim, and C. R. Giardina, "A robust digital baseband predistorter constructed using memory polynomials," *IEEE Trans. Commun.*, vol. 52, no. 1, pp. 159–165, Jan. 2004.

[15] A. Zhu, P. J. Draxler, J. J. Yan, T. J. Brazil, D. F. Kimball, and P. M. Asbeck, "Open-loop digital predistorter for RF power amplifiers using dynamic deviation reduction-based volterra series," *IEEE Trans. Microw. Theory Techn.*, vol. 56, no. 7, pp. 1524–1534, Jul. 2008.

[16] W. H. Doherty, "A new high-efficiency power amplifier for modulated waves," *Bell Syst. Tech. J.*, vol. 15, no. 3, pp. 469–475, Jul. 1936.

[17] D. Gustafsson, J. C. Cahuana, D. Kuylenstierna, I. Angelov, and C. Fager, "A GaN MMIC modified Doherty PA with large bandwidth and reconfigurable efficiency," *IEEE Trans. Microw. Theory Techn.*, vol. 62, no. 12, pp. 3006–3016, Dec. 2014.

[18] F. Giannini, P. Colantonio, and R. Giofre, "The Doherty amplifier: Past, present & future," in *Proc. Integr. Nonlinear Microw. Millimetre-Wave Circuits Workshop (INMMiC)*, Oct. 2015, pp. 1–4.

[19] D. Cox, "Linear amplification with nonlinear components," *IEEE Trans. Commun.*, vol. COM-22, no. 12, pp. 1942–1945, Dec. 1974.

[20] T. W. Barton and D. J. Perreault, "Theory and implementation of RF-input outphasing power amplification," *IEEE Trans. Microw. Theory Techn.*, vol. 63, no. 12, pp. 4273–4283, Dec. 2015.

[21] F. Wang, D. F. Kimball, D. Y. Lie, P. M. Asbeck, and L. E. Larson, "A monolithic high-efficiency 2.4-GHz 20-dBm SiGe BiCMOS envelope-tracking OFDM power amplifier," *IEEE J. Solid-State Circuits*, vol. 42, no. 6, pp. 1271–1281, Jun. 2007.

[22] Y. Li, J. Lopez, P.-H. Wu, W. Hu, R. Wu, and D. Y. C. Lie, "A SiGe envelope-tracking power amplifier with an integrated CMOS envelope modulator for mobile WiMAX/3GPP LTE transmitters," *IEEE Trans. Microw. Theory Techn.*, vol. 59, no. 10, pp. 2525–2536, Oct. 2011.

[23] Z. Wang, "Demystifying envelope tracking: Use for high-efficiency power amplifiers for 4G and beyond," *IEEE Microw. Mag.*, vol. 16, no. 3, pp. 106–129, Apr. 2015.

[24] P. Montezuma, M. Beko, R. Dinis, J. Guerreiro, and P. Viegas, "Apparatus for quantized linear amplification with nonlinear amplifiers," USPTO Patent 10 069 467 B1, Sep. 4, 2018.

[25] P. Viegas, J. Guerreiro, H. Serra, R. Madeira, R. Laires, P. Morgado, R. Dinis, P. Montezuma, and J. P. Oliveira, "A highly-efficient amplification scheme for OFDM signals," in *Proc. VTC Spring Conf.*, Feb. 2021.

[26] T. Araújo and R. Dinis, *Analytical Evaluation of Nonlinear Distortion Effects on Multicarrier Signals*. Boca Raton, FL, USA: CRC Press, 2015.

[27] *ETSI Technical Specification (TS)*, Standard 138 101-1 V15.3.0, Oct. 2018.

[28] M. McKinley, K. A. Remley, M. Myslinski, J. S. Kenney, D. Schreurs, and B. Nauwelaers, "EVM calculation for broadband modulated signals," in *Proc. 64th ARFTG Conf.*, Orlando, FL, USA, Dec. 2004, pp. 45–52.

[29] N. O. Sokal and A. D. Sokal, "Class E—A new class of high-efficiency tuned single-ended switching power amplifiers," *IEEE J. Solid-State Circuits*, vol. SSC-10, no. 3, pp. 168–176, Jun. 1975.

[30] E. J. Wilkinson, "An N-Way hybrid power divider," *IEEE Trans. Microw. Theory Techn.*, vol. MTT-8, no. 1, pp. 116–118, Jan. 1960.

[31] *RF Wireless World*. Accessed: Mar. 2021. [Online]. Available: https://www.rfwireless-world.com/test-andmeasurement/IEEE-802-11ax-EVM.html

[32] Y. Liu, X. Tang, G. Mangraviti, K. Khalaf, Y. Zhang, W.-M. Wu, S.-H. Chen, B. Debaillie, and P. Wambacq, "A 28 GHz front-end module with T/R switch achieving 17.2 dBm P_{sat}, 21.5% PAE_{max} and 3.2 dB NF in 22 nm FD-SOI for 5G communication," in *Proc. IEEE Radio Freq. Integr. Circuits Symp. (RFIC)*, Aug. 2020, pp. 347–350.

[33] A. Banerjee, L. Ding, and R. Hezar, "A high efficiency multi-mode outphasing RF power amplifier with 31.6 dBm peak output power in 45nm CMOS," *IEEE Trans. Circuits Syst. I, Reg. Papers*, vol. 67, no. 3, pp. 815–828, Mar. 2020.

[34] S. Hu, S. Kousai, and H. Wang, "A broadband mixed-signal CMOS power amplifier with a hybrid class-G Doherty efficiency enhancement technique," *IEEE J. Solid-State Circuits*, vol. 51, no. 3, pp. 598–613, Mar. 2016.

[35] E. Kaymaksut and P. Reynaert, "Dual-mode CMOS Doherty LTE power amplifier with symmetric hybrid transformer," *IEEE J. Solid-State Circuits*, vol. 50, no. 9, pp. 1974–1987, Sep. 2015.

[36] Y. H. Chee, F. Golcuk, T. Matsuura, C. Beale, J. F. Wang, and O. Shanaa, "17.1 A digitally assisted CMOS WiFi 802.11ac/11ax front-end module achieving 12% PA efficiency at 20dBm output power with 160MHz 256-QAM OFDM signal," in *IEEE Int. Solid-State Circuits Conf. (ISSCC) Dig. Tech. Papers*, Feb. 2017, pp. 292–293.

[37] K. Kim and C. Nguyen, "A 16.5–28 GHz 0.18-μm BiCMOS power amplifier with flat 19.4 $\pm$ 1.2 dBm output power," *IEEE Microw. Wireless Compon. Lett.*, vol. 24, no. 2, pp. 108–110, Feb. 2014.
[38] C. Y. Law and A.-V. Pham, "A high-gain 60GHz power amplifier with 20dBm output power in 90nm CMOS," in *IEEE Int. Solid-State Circuits Conf. (ISSCC) Dig. Tech. Papers*, Feb. 2010, pp. 426–427.
[39] J.-W. Lai and A. Valdes-Garcia, "A 1V 17.9dBm 60GHz power amplifier in standard 65nm CMOS," in *Proc. IEEE Int. Solid-State Circuits Conf. (ISSCC)* Feb. 2010, pp. 424–425.

PEDRO VIEGAS received the M.Sc. degree in electrical and computer engineering from the Faculdade de Ciências e Tecnologia da Universidade Nova de Lisboa (FCT–UNL), in 2017. He is currently pursuing the master's degree in applied business management from the Nova School of Business and Economics (SBE). From January 2018 to April 2019, he was an IT Researcher with the Instituto de Telecomunicações, where he was working on projects, such as multilayer massive MIMO systems for the fifth generation (5G) wireless communications (MM5G) and power-efficient solutions for secure wireless sensor networks (PES3N). Since May 2019, he has been a Signal Processing Engineer with Koala Tech, where he is working on multi-branch amplification structures and quantized amplification schemes, multi-carrier/single-carrier signals, and M-QAM signal modulation. At Koala Tech, he is also a Founding Member, a Marketing Coordinator, and an Internationalization Coordinator. He received the Project Management Training Certificate from Nova SBE.

HUGO SERRA received the M.Sc. and Ph.D. degrees in electrical and computer engineering (ECE) from the Faculty of Sciences and Technology (FCT), NOVA University of Lisbon (NOVA), Portugal, in 2012 and 2017, respectively. He was a Researcher with the Centre for Technology and Systems (CTS) UNINOVA, from 2013 to 2018. Since January 2019, he has been a Researcher with the Radio Systems Group, Instituto de Telecomunicações (IT).

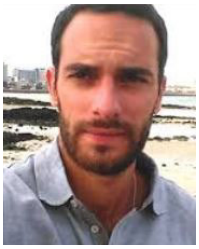

JOÃO GUERREIRO (Member, IEEE) received the M.Sc. and Ph.D. degrees in electrical and computer engineering from the Faculdade de Ciências e Tecnologias da Universidade Nova de Lisboa, in 2012 and 2016, respectively. Since 2012, he has been actively involved in scientific research in the field of wireless communications. He is currently an Invited Assistant Professor with the Faculdade de Ciências e Tecnologias da Universidade Nova de Lisboa and a Researcher with the Instituto de Telecomunicações. Since 2018, he has been one of the founders of Koala Tech. He has participated in several national and international research projects in the last years. He published more than 20 journal articles, 40 conference articles (one Best Paper Award), three patents (granted or pending), and one book chapter.

RICARDO MADEIRA received the M.Sc. degree in electrical and computer engineering (ECE) from the NOVA Faculty of Science and Technology (NOVA FCT), Lisbon, in 2015, where he is currently pursuing the Ph.D. degree in ECE. He has been a Researcher with the Centre of Technology and Systems (CTS), since 2015, where he has been involved in the design of mixed-signal integrated circuits (ICs) in nanoscale CMOS technology, namely the design and optimization of a fully integrated power management unit (PMU) with switched capacitor (SC) DC-DC converters.

DAVID BORGES was born in Almada, Portugal, in 1993. He received the B.Sc. and M.Sc. degrees in electrical and computer engineering from the Faculty of Science and Technology, Nova University, Caparica, Portugal, in 2014 and 2017, respectively. He is currently pursuing the Ph.D. degree in electrical and computer engineering in the field of telecommunication. From 2016 to 2018, he worked as a Consultant of cloud infrastructure services for an IT company in Oeiras, Portugal. His current research interests include wireless communication, signal processing, multi-antenna transmission (MIMO & massive MIMO), precoding techniques, and interference cancelation.

RUI DINIS (Senior Member, IEEE) received the Ph.D. degree from the Instituto Superior Técnico (IST), Technical University of Lisbon, Portugal, in 2001, and the Habilitation degree in telecommunications from the Faculdade de Ciências e Tecnologia (FCT), Universidade Nova de Lisboa (UNL), in 2010. He was a Researcher with the Centro de Análise e Processamentode Sinal (CAPS), IST, from 1992 to 2005, and a Researcher with the Instituto de Sistemas e Robótica (ISR), from 2005 to 2008. From 2001 to 2008, he was a Professor with IST. In 2003, he was an Invited Professor with Carleton University, Ottawa, Canada. Since 2009, he has been a Researcher with the Instituto de Telecomunicações (IT). He is currently an Associate Professor with the FCT–UNL. He has been actively involved in several international research projects in the broadband wireless communications area, such as RACE project MBS, ACTS project SAMBA, and IST projects B-BONE and C-MOBILE, and many national projects, most of them as a nuclear researcher and/or in charge of his research center in multi-institutional projects. He was involved in pioneer projects on the use of mm-waves for broadband wireless communications (international projects MBS and SAMBA). He has published six books, over 100 journal articles and book chapters, and over 300 conference papers (of which five received best papers' awards), and over 18 patents (attributed or pending). His main research activities are on modulation and transmitter design, nonlinear effects on digital communications and receiver design (detection, equalization, channel estimation and carrier synchronization), with emphasis on frequency-domain implementations, namely for MIMO systems and/or OFDM and SC-FDE modulations. He is also working on cross-layer design and optimization involving PHY, MAC, and LLC issues, and indoor positioning techniques. He is or was with the Organizing Committee of several international conferences, such as the IEEE conferences ICT'2014, VTC'2017-Fall, VTC'2018-Spring, and ISWCS'2018. He is also the President of VTS Portugal Chapter, since 2016 and a member of several technical committees of the IEEE Communications Society, such as SPCE, RCC, WC, and CT. He is an Editor of IEEE TRANSACTIONS ON WIRELESS COMMUNICATIONS, IEEE TRANSACTIONS ON COMMUNICATIONS, IEEE TRANSACTIONS ON VEHICULAR TECHNOLOGY and *Physical Communication* (Elsevier).

PAULO MONTEZUMA (Member, IEEE) received the Ph.D. and the master's degree in telecommunications with the Faculdade de Ciências e Tecnologia (FCT), Universidade Nova de Lisboa (UNL). He was a Researcher with the Centro de Análise e Processamentode Sinal (CAPS), IST, from 1997 to 2005. Since 2013, he has been a Researcher with the Instituto de Telecomunicações (IT). Since 2018, he has also been one of the founders of Koala Tech, where he is currently the CEO of the company. He is currently an Associate Professor with the Faculdade de Ciências e Tecnologia (FCT), Universidade Nova de Lisboa (UNL). He has been actively involved in several international research projects in the broadband wireless communications area and many national industrial and research projects most of them as a nuclear researcher and/or in charge of his research center. He published over 44 journal articles and four book chapters, one book, and more than 120 conference papers (one Best Paper Award), has assigned 18 patents and three pending. His main research activities are on modulation and transmitter design, coding, nonlinear effects on digital communications and receiver design, with emphasis on frequency-domain implementations, namely for MIMO systems and/or OFDM and SC-FDE modulations and energy efficient transmission techniques. He is an editor of several journals.

JOÃO PEDRO OLIVEIRA (Member, IEEE) received the M.Sc. and Ph.D. degrees in microelectronics and telecommunications from the Department of Electrical and Computer Engineering, Nova University of Lisbon. He has more than 23 years of experience in the field, including professional, business management, and academic activities. He has five years of experience in telecommunications companies, where among other functions, he was fully involved in the development and deployment of the first 3G radio networks. In 2003, he co-founded the Mobbit Systems Company, where he was an Active Member of the Management Board for more than ten years, and the CSO responsible for the product technical development, both hardware and software. A development strategy strongly focused on the market permitted the company to reach the leadership in the area and in the country. He is currently a Professor of integrated microelectronics with the Department of Electrical and Computer Engineering, Nova University of Lisbon. He is also a Senior Researcher with the Centre of Technology and Systems-CTS, where he has been involved in the design of mixed-signal integrated circuits in nanoscale CMOS technology, namely radio frequency circuits for the telecommunications. He published over 30 articles in international journals and over 30 papers in international leading conferences and has authored one book and has four patents pending. He is a member of the Circuits and Systems Society (CASS), the Solid-State Circuits Society (SSCS), the IEEE Communications Society (ComSoc), the IEEE Microwave Theory and Techniques Society (MTT-S), and the IEEE Computer Society. He is the Chair of the IEEE Solid-State Society Chapter of the IEEE Portugal Section.

LUÍS M. CAMPOS received the B.Tech. degree from the Instituto Superior Técnico (IST), Lisbon, in 1992, the M.S. degree in information and computer science from the University of California at Irvine, Irvine, in 1995, and the Ph.D. degree in information and computer science, in 1999. He worked as a Faculty Member of the University of California at Irvine, an Intern with NASA, as a Researcher with INESC, and as a Teaching Assistant with the Instituto Superior Técnico. With 25 years of experience managing companies from the startup stage to medium size, he is focused on creating a self-sustainable virtuous cycle ecosystem of business angels funds, venture capital funds, active investors, researchers, and entrepreneurs, which will cover all stages of creation and growth until IPO. He serves as an Expert Evaluator for the European Commission, leads the Business Angel Fund SMENT Digital and serves on the board of over ten companies. He has founded and led several companies, some of which have been sold to much large companies, namely ZPX Interactive Software. He currently leads the Research and Development Team, PDM&FC. He is also the Managing Director of Koala Tech and responsible for worldwide investment funding. He is involved in 12 European funded research projects (Horizon2020) and five national research projects (Portugal2020). He has published dozens of papers in international conferences in areas as diverse as parallel computing, agent-based computing, resource management in distributed systems, simulation theory, cluster computing and grid computing, computer vision, information systems, and e-Government. Some companies have received the Prestigious Award Deloitte Technology Fast 500, namely Go4Mobility, and some have been selected by the Portuguese state as one of the most innovative companies in the country, namely PDMFC.

MARKO BEKO was born in Belgrade, Serbia, in November 1977. He received the Ph.D. degree in electrical and computer engineering from the Instituto Superior Técnico (IST), Universidade de Lisboa, Portugal, in 2008. He received the title of the Professor with Aggregation/Habilitation of electrical and computer engineering from the Universidade Nova de Lisboa, Lisbon, in 2018. He is currently an Associate Professor with IST. He is also one of the founders of Koala Tech. He has published 60 journal articles, 85 conference papers, three book chapters, and one book. He holds eight patents (granted and pending) in USA and Portugal. His current research interests include the area of signal processing for wireless communications. He serves as an Associate Editor for the IEEE Open Journal of the Communications Society and Journal on *Physical Communication* (Elsevier). He was the winner of the 2008 IBM Portugal Scientific Award. According to the methodology proposed by Stanford University, he was among the most influential researchers in the world, in 2019, where he joined the top 1 of scientists whose work is most cited by other colleagues in the field of information and communication technologies, sub-area networks and telecommunications.